DMD Fast Forward. Published on November 17, 2011 as doi: 10.1124/dmd.111.041665
This article has not been copyedited and formatted. The final version may differ from this version.

Title Page

Predicting phenolic acid absorption in Caco-2 cells: a theoretical permeability model & mechanistic study

Authors: Tracy L Farrell, Laure Poquet, Tristan P Dew, Stuart Barber, Gary Williamson

Affiliations: School of Food Science and Nutrition, University of Leeds, UK (T.F., T.P.D., G.W.). Department of Statistics, University of Leeds, UK (S.B). Nestlé Research Center, Vers-chez-les-Blanc, Lausanne, Switzerland (L.P., G.W.).

DMD Fast Forward. Published on November 17, 2011 as DOI: 10.1124/dmd.111.041665
This article has not been copyedited and formatted. The final version may differ from this version.

Running Title Page

Running title: Predictive absorption of phenolic acids by theoretical modeling

Address correspondence to: Prof. G. Williamson, School of Food Science and Nutrition, University of Leeds, UK. Email: g.williamson@leeds.ac.uk. Tel: +44 (0)113 343 8380.

Content:

Number of text pages: 35

Number of table: 5

Number of Figs: 8

Number of references: 40

Word count:

Abstract: 203

Introduction: 475

Discussion: 1481

Non Standard Abbreviations:

CGAs: chlorogenic acids; CQA: caffeoylquinic acid; DAD: diode array detector; diCQA: di-*O*-caffeoylquinic acid; DMEM: Dulbecco's modified Eagle's medium; DMSO: dimethyl sulfoxide; FQA: feruloylquinic acid; HBSS: Hank's balanced salts solution; HCAs: hydroxycinnamic acids; HPLC: high-performance liquid chromatography; Log *D*: distribution coefficient in 1-octanol/ water; MW: molecular weight; P_{app}: experimental apparent permeability coefficient; P_{app}^{trans} : predicted transcellular permeability; TEER: trans-epithelial electrical resistance; TTP: theoretical transcellular permeability.

DMD Fast Forward. Published on November 17, 2011 as DOI: 10.1124/dmd.111.041665
This article has not been copyedited and formatted. The final version may differ from this version.

Abstract

There is a considerable need to rationalize the membrane permeability and mechanism of transport for potential nutraceuticals. The aim of this investigation was to develop a theoretical permeability equation, based on a reported descriptive absorption model, enabling calculation of the transcellular component of absorption across Caco-2 monolayers. Published data for Caco-2 permeability of 30 drugs transported by the transcellular route was correlated with the descriptors 1-octanol/ water distribution coefficient (Log *D*, pH 7.4) and size, based on molecular weight (MW). Non-linear regression analysis was used to derive a set of model parameters *a'*, *β'* and *b'* with an integrated molecular weight function. The new theoretical transcellular permeability (TTP) model obtained a good fit of the published data ($R^2 = 0.93$), and predicted reasonably well ($R^2 = 0.86$) the experimental apparent permeability coefficient (P_{app}) for 9 non-training set compounds reportedly transported by the transcellular route. For the first time, the TTP model was used to predict the absorption characteristics of 6 phenolic acids and this original investigation was supported by *in vitro* Caco-2 cell mechanistic studies, which suggested that deviation of the P_{app} value from the predicted transcellular permeability (P_{app}^{trans}) may be attributed to involvement of active uptake, efflux transporters or paracellular flux.

DMD Fast Forward. Published on November 17, 2011 as DOI: 10.1124/dmd.111.041665
This article has not been copyedited and formatted. The final version may differ from this version.

Introduction

A growing number of epidemiological studies indicate an association between habitual coffee consumption and reduced risk of type 2 diabetes (van Dam and Hu, 2005). Coffee is a predominant source of phenolic acids in the form of hydroxycinnamic acids (HCAs) such as caffeic acids and ferulic acids, typically linked to a quinic acid moiety to form a subgroup known as chlorogenic acids (CGAs). CGAs and HCA derivatives may play an important role in biological mechanisms (Wang et al., 2008;Henry-Vitrac et al., 2010) with potential health benefits. Despite these reported pharmacological effects, the mechanism of intestinal absorption has been elucidated for only a small number of phenolic acids (Konishi and Kobayashi, 2004;Poquet et al., 2008). There is a considerable need for rationalizing intestinal permeability of phenolic acids because it is a critical step towards understanding their potential bioactivity. The Caco-2 cell line has been widely employed as a model of intestinal absorption and estimate of oral bioavailability (Artursson et al., 2001). However, when investigating the complex mixture of compounds present in foods the number of permeability studies required creates several financial and technical challenges, and clarification of absorption pathways remains a labor intensive and difficult task. The ability to make *in silico* predictions of the permeability of dietary components based on physicochemical properties would streamline the high-throughput screening of potential bioactives and provide an estimation of the major pathway of permeation and bioavailability.

Theoretical models of permeation through *in vitro* biological membranes such as the human intestine (Camenisch et al., 1998) have been developed within the pharmaceutical sciences. In principle these models correlate passive intestinal permeability with physicochemical attributes (descriptors) to estimate the absorption of similar compounds. Most models assume transport can occur through two main pathways: via the restricted aqueous spaces between cells (*paracellular*), and through the cell membrane (*transcellular*). Passive diffusion can be considered as the predominant mechanism of permeation for ingested compounds. Diffusion processes are largely governed by inter-related physicochemical descriptors: lipophilicity, polarity (charge, hydrogen bonding, polar surface area) (van de Waterbeemd, 1998) and molecular weight (Camenisch et al., 1998) as described by Fick's First Law of diffusion. Involvement of metabolism by cytochrome P450 enzymes and efflux processes and active transport may limit or improve membrane uptake respectively, causing deviation from the predicted permeability.

Theoretical models are a useful tool for high-throughput screening of potentially bioavailable compounds, but have never been used to investigate absorption characteristics of polyphenols. In the current study we have refined a previously reported descriptive absorption model, which related permeation across a biological

membrane to lipophilicity measured as the distribution coefficient (Log *D*) and molecular weight (MW) (Camenisch et al., 1998). For the first time, the new theoretical transcellular permeability (TTP) model was used to estimate the transcellular passive diffusion component for an external validation set consisting of 22 compounds, including a range of phenolic acids of diverse MW.

DMD Fast Forward. Published on November 17, 2011 as DOI: 10.1124/dmd.111.041665
This article has not been copyedited and formatted. The final version may differ from this version.

Materials and Methods

Chemicals

Compounds used in this study were obtained from Sigma-Aldrich (Dorset, UK) unless stated otherwise. All water refers to deionized Millipore water, Millipore UK Ltd (Hertfordshire, UK). Culture flasks, Transwell plates fitted with polycarbonate semipermeable membranes of 0.4 μm pore size and 4.67 cm^2 area were manufactured by Corning Life Sciences and supplied by Sigma-Alrich (Dorset, UK). 5-*O*-caffeoylquinic acid (5-*O*-CQA) and 3,5-di-*O*-caffeoylquinic acid (3,5-*O*-diCQA) were purchased from Biopurify Pharmaceuticals Ltd (Sichuan, China). Standard 5-*O*-feruloylquinic acid (5-*O*-FQA) was synthesized at the Nestlé Research Center (Lausanne, Switzerland) and kindly donated by D. Barron.

Selection of the Training and Validation Set Compounds

This study utilized an existing data set with a previously reported passive permeability-lipophilicity relationship (Artursson and Karlsson, 1991;Camenisch et al., 1998). However, our aim was to develop a theoretical permeability equation to predict absorption exclusively via passive *transcellular* diffusion, referred to as the theoretical transcellular permeability (TTP) model. Thus, a literature search was performed to filter compounds reported to have extensive active or efflux transport, metabolism or uptake by the paracellular route. Since transport of a single compound across the intestinal barrier may involve absorption via several routes (Avdeef and Tam, 2010;Sugano et al., 2010), it is a difficult task to identify compounds with transport wholly by the transcellular route. However, based on the following evidence the compounds present in the training set are *mainly transported* via the passive transcellular pathway. This conclusion was based on reported insensitivity to membrane junction tightness (Hilgendorf et al., 2000), *in vitro* mechanistic studies, which correct for the contribution of paracellular component of transport (Avdeef and Tam, 2010), *ex vivo* tissue transport studies (Bernards and Hill, 1992;Kern and Bernards, 1997), theoretical modeling based on pH partition theory (Obata et al., 2005), and human bioavailability data (Artursson and Karlsson, 1991;Palm et al., 1997;Yamashita et al., 2000) indicating rapid and significant absorption (greater than 50% of oral dose). The following compounds were selected as model compounds transported by mainly transcellular passive diffusion (n = 30): Alprenolol, antipyrine, ceftriaxone, corticosterone, coumarin, dexamethasone, diazepam, epinephrine, felodipine, guanabenz, guanoxan, hydrocortisone, imipramine, ketoprofen, lidocaine, metoprolol, mibefradil, morphine, nitrendipine, phenytoin, piroxicam, practolol, propranolol, remikiren, sulpiride, testosterone, theophylline, tiacrilast, verapamil and warfarin.

DMD Fast Forward. Published on November 17, 2011 as DOI: 10.1124/dmd.111.041665
This article has not been copyedited and formatted. The final version may differ from this version.

In order to evaluate the capacity of the TTP model to predict the transcellular component of permeability across Caco-2 monolayers for compounds outside of the training set, P_{app}^{trans} values were calculated for a total of 22 non-training set compounds of known transport mechanism consisting of 6 phenolic acids and 9 transcellular compounds: acetylsalicylic acid, aminopyrine, 5-*O*-caffeoylquinic acid, caffeic acid, caffeine, carbamazepine, ferulic acid, 3,5-di-*O*-caffeoylquinic acid, 3,4-dimethoxycinnamic acid, 5-*O*-feruloylquinic acid, fluvastatin, griseofulvin, naproxen, nevirapine, and salicylic acid. Mannitol was used as the classic paracellular marker. D-glucose (GLUT2), Gly-pro (dipeptide transporter) and L-dopa (amino acid transporter) were chosen as model compounds taken up by specific transporters. Cimetidine, rhodamine 123 and talinolol have been reported as a substrate for the efflux transporter P-glycoprotein (Hilgendorf et al., 2000; Troutman and Thakker, 2003).

Inter-laboratory variability

In brief, Caco-2 permeability studies and Log *D* measurements were performed as described below using acetylsalicylic acid, alprenolol, atenolol, hydrocortisone, metaprolol and salicylic acid to determine the extent of variability between our findings and the original published data for the training set (Artursson and Karlsson, 1991). Data are presented as mean ± S.D.

Determination of distribution coefficient

Log *D* values were determined for acetylsalicylic acid, alprenolol, atenolol, caffeic acid, 5-*O*-CQA, 3,4-dimethoxycinnamic acid, 3,5-diCQA, ferulic acid, 5-*O*-FQA, hydrocortisone, metaprolol and salicylic acid by the 1-octanol/ water shake flask method as described in detail previously (Farrell et al., 2011). Each compound was identified by retention time and UV spectra relative to authentic standards and the Log *D* determined as the mean of 10 replicates.

Cell culture

The human colon adenocarinoma cell line, Caco-2 (HTB-37) was obtained from the American Type Culture Collection at passage 25 (LGC Promochem, Middlesex, UK). Permeability studies utilized Caco-2 cells between passages 30 and 50. Caco-2 cells were added to Transwell inserts (24 mm diameter, 4.67 cm^2 growth area) at a density 6 x 10^4 cells/cm^2 and cultured for 21 d at 37°C under a humidified atmosphere of 95% air: 5% CO_2. The culture medium, DMEM supplemented with 10% fotal bovine serum, 584 mg/l L-glutamine, 100U/ml penicillin-streptomycin, 1% (v/v) minimum essential medium and 0.25 µg/ml amphotericin B was replaced every other day.

DMD Fast Forward. Published on November 17, 2011 as DOI: 10.1124/dmd.111.041665
This article has not been copyedited and formatted. The final version may differ from this version.

Permeability and mechanistic studies

On or after 22 d, permeability studies were initiated by careful aspiration of the culture medium from apical and basal compartments and 2 ml of modified HBSS, consisting of HBSS containing 1.8 mM calcium chloride (pH 7.4), was added to each compartment. Plates were incubated at 37 °C in a humidified 5% CO_2 atmosphere for 15 min to allow equilibration of tight junction integrity. Apical and basal solutions were carefully aspirated and 2 ml of apical transport solution (pH 7.4) was added to the apical compartment, all basal solutions were modified HBSS (pH 7.4). Thus, both donor and receiver compartments used the same pH, which was a pre-assumption of the permeability-lipophilicity model described by Camenisch et al. (1998). The transport solution consisted of modified HBSS (pH 7.4) containing 500 μM of test compound, which was similar to the amount used to determine P_{app} values for the training set compounds. A concentrated stock of test compound, which was either atenolol, alprenolol, 5-*O*-CQA, caffeic acid, 3,5-diCQA, 3,4-dimethoxycinnamic acid, ferulic acid, 5-*O*-FQA, hydrocortisone, metaprolol or salicylic acid was prepared in DMSO, then diluted in modified HBSS by 500-fold so that the percentage of DMSO was maintained at 0.2% in each transport experiment. Measurement of the trans-epithelial electric resistance (TEER) was taken with a Millicell ERS volt-ohm meter fitted with a chopstick probe (Millipore Ltd, Watford, UK). Plates containing differentiated monolayers and a reference sample (2 ml) of transport solution in a cell free compartment were incubated at 37 °C in a humidified 5% CO_2 atmosphere for 1 h without stirring. Permeation was monitored by removal of basal solution (100 μl) at 30, 60, 90, 120 min, and the volume was replaced with modified HBSS. At the end of the incubation period, TEER measurements were repeated, an aliquot (1 ml) was removed from the apical and basal compartments to which acetic acid was added to obtain a final concentration of 10 mM and samples stored at -80°C. In all transport experiments the pH measurements were recorded on the initial transport solution and repeated for all apical and basal compartment solutions at the end of the incubation period.

To assess the time-dependent transport of 5-*O*-CQA, 5-*O*-FQA and 3,5-diCQA, permeability studies were performed in the A→B (apical to basal) and B→A (basal to apical) directions (bi-directional). In brief, transport solution (pH 7.4) consisting of test compound (500 μM) prepared from a concentrated DMSO stock and diluted in modified HBSS containing 1.8 mM calcium chloride was added (2 ml) to the donor compartment, and all receiver solutions (2 ml) were modified HBSS (pH 7.4). Samples were removed at 30, 60, 90, 120 min and stored as described above.

Concentration dependence of membrane permeability was investigated for 5-*O*-CQA, 5-*O*-FQA and 3,5-diCQA by bi-bidirectional permeability studies using test compound at a final concentration of 50 μM, 100 μM, 200 μM and 500 μM prepared from a concentrated DMSO stock as described above. In brief, transport solution

DMD Fast Forward. Published on November 17, 2011 as DOI: 10.1124/dmd.111.041665
This article has not been copyedited and formatted. The final version may differ from this version.

(pH 7.4) consisting of test compound diluted in HBSS containing 1.8 mM calcium chloride was added (2 ml) to the donor compartment, modified HBSS (pH 7.4) was used as the receiver solution (2 ml), Transwells containing differentiated monolayers were incubated for 1 h and thereafter samples (1 ml) were removed from the receiver compartment and stored as described.

Mechanistic studies were performed to elucidate the role of tight junction integrity on phenolic acid permeability across the Caco-2 monolayer. In brief, inserts containing differentiated monolayers (n = 3 per condition) were aspirated to remove apical and basal medium and replaced (2 ml) with HBSS (pH 7.4) containing either 18 μM or 3.6 mM calcium chloride and incubated at 37 °C in a humidified 5% CO_2 atmosphere for 15 min to vary the monolayer resistance. After 15 min both compartments were carefully aspirated and transport solution (2 ml) consisting of 500 μM test compound and HBSS (pH 7.4) at the necessary calcium chloride concentration was added to the apical compartment, HBSS (pH 7.4) of the same calcium chloride concentration was added (2 ml) to the basal compartment. TEER measurements were recorded and the plates were incubated at 37 °C in a humidified 5% CO_2 atmosphere for 1 h without stirring. After 1 h, TEER measurements were repeated and samples (1 ml) were collected from both compartments and stored as described above. TEER values were corrected for the intrinsic cell-free resistance of the insert in all cell culture studies.

To investigate the involvement of passive diffusion in the absorption process, the bi-directional permeation was evaluated. In brief, differentiated monolayers were incubated with transport solution consisting of HBSS containing 500 μM test compound and 1.8 mM calcium chloride added either to the apical or basal compartment depending on the direction of transport, modified HBSS (pH 7.4) was the receiver solution. Plates were incubated for 1 h and the amount permeating to the receiver compartment was determined by HPLC-DAD. The efflux ratio for permeability was calculated to identify non-passive transport mechanisms.

To study the role of ABC transporters on absorption, differentiated Caco-2 monolayers were exposed to 3,5-diCQA (500 μM) in the basal compartment and 25 μM or 10 μM of an inhibitor in the apical compartment. Both test compound and inhibitor were prepared from a concentrated DMSO stock and diluted in modified HBSS containing 1.8 mM calcium chloride, the final percentage of DMSO in all the experiments was maintained at 0.2% basal and 0.05% apical. The amount of 3,5-diCQA detected in the apical compartment after incubation (1 h) at 37 °C, 5% CO_2 was compared to the amount detected under control conditions, which was the absence of inhibitor. P_{app} values were determined for control and inhibitors conditions and the percentage inhibition was calculated as the difference between the P_{app} for control and inhibitor, divided by the P_{app} for control, multiplied

DMD Fast Forward. Published on November 17, 2011 as DOI: 10.1124/dmd.111.041665
This article has not been copyedited and formatted. The final version may differ from this version.

by 100. Inhibitors were used at similar concentrations to those often effective in inhibition studies and have been demonstrated to potently inhibit ABC transporter proteins: the role of breast cancer resistance protein (BCRP, ABCG2) was investigated using apigenin; P-glycoprotein (P-gp, ABCB1) mediated transport was studied with cyclosporine A; involvement of multi-drug resistance-associated protein (MRP2 ABCC2) was analyzed using MK 571, and quercetin was used as a combined inhibitor of all 3 ABC transporters.

Deproteination of culture media

Transport solutions were thawed and extracted as described previously (Farrell et al., 2011). In brief, transport solutions (46 µl) were combined with 6.4 µl of 50% aqueous formic acid, ascorbic acid (final concentration 1 mM) and sinapic acid (final concentration 50 µM) as an internal standard. To the mixture, 112.5 µl of acetonitrile was added drop wise to precipitate proteins and the samples were vortexed for 1 min and allowed to stand (1 min), this procedure was repeated 2 times before centrifugation at 17,000 × g for 5 min. The supernatant (150 µl) was removed and dried under centrifugal evaporation (Genevac EZ-2 plus, Suffolk, UK). Dried samples were reconstituted in 50 µl of water containing acetonitrile (v/v, 5:95) and analyzed by HPLC using a diode array detector (DAD).

HPLC-DAD Analysis

Reconstituted samples were injected on to a Rapid Resolution HPLC with DAD fitted with a deuterium lamp, semi-micro flow cell (6 mm pathlength), (1200 series Agilent Technologies, Berkshire, UK). Elution was achieved at 30 °C on an Eclipse plus C18 column (2.1 mm × 100 mm, 1.8 µm; Agilent Technologies, Berkshire, UK) using a 60 min gradient of (A) premixed water containing acetonitrile (v/v, 95:5) and (B) premixed acetonitrile containing water (v/v, 95:5) both containing 0.1% formic acid at a flow rate of 0.26 ml/min. Elution was initiated at 0% of solvent B and maintained for 17 min; the percentage of solvent B was then increased to 16% over the next 21 min and increased to 100% for 5 min before initial starting conditions were resumed for a 15 min column re-equilibration.

Recovery efficiency

Recovery efficiency experiments were performed for caffeic acid, 5-*O*-CQA, 3,5-diCQA, 3,4-dimethoxycinnamic acid, ferulic acid, and 5-*O*-FQA in the absence of cells and used as a correction factor in quantification. In brief, test phenolic acids, prepared from a concentrated stock in DMSO, were diluted with HBSS (pH 7.4) to 10 µM and the final percentage of DMSO was 0.2%. Samples were incubated for 2 h at 37 ºC in the absence of cells in Transwell plates. After incubation, a portion (100 µl) was removed, deproteinated as described above and the recovery determined by HPLC-DAD (n = 10).

DMD Fast Forward. Published on November 17, 2011 as DOI: 10.1124/dmd.111.041665
This article has not been copyedited and formatted. The final version may differ from this version.

Data analysis

P_{app} values were either taken from the literature or determined in this study by HPLC-DAD quantification of the concentration of compound in the receiver compartment following transport across the Caco-2 monolayer. The calculation was described by the following equation,

$$P_{app} = \frac{V_D}{A \times M_D} \times \frac{dM_R}{dt} \qquad \textit{(eq. 1)}$$

where V_D = apical donor volume (cm^3), A = membrane surface area (cm^2), dM_R/dt = change in the amount (mol) of compound in the basal receiver compartment over time (sec). M_D was the initial amount of compound in the apical donor compartment at time 0, which was determined from the reference sample of the transport solution. Values of P_{app} are only valid under experimental conditions that provide a constant concentration gradient, that is, the basal receiver amount should not exceed 10% of the amount in the apical compartment (Hubatsch et al., 2007). Therefore, sampling intervals in this study (30, 60, 90, 120 min) were selected to accommodate slow and rapid transport characteristics. For most compounds, the dM_R was measured as the amount of compound accumulated at the end of the 60 min or for rapidly permeated compounds before more than 10% of the compound had permeated to the basal receiver compartment and thus sink conditions were preserved. The amount transported to the basal compartment was less than 10% for all compounds except for metaprolol and alprenolol where transport was less than 15%.

Mass balance, defined as the sum of the amounts of compound recovered in the apical and basal compartments at the end of the transport experiment, as a percentage of the initial apical donor amount, was calculated for each transport study using the following equation,

$$\textit{Mass Balance \%} = \left(\left(M_{D(fin)} + \sum M_{s(t)} + M_{R(fin)}\right) / M_{A(0)}\right) \times 100 \qquad \textit{(eq. 2)}$$

where M_D and M_R are the amounts in the donor and receiver compartment (mol) at the start (0) and end (fin) of the experiment, and $M_{s(t)}$ was the amount withdrawn in samples removed at time intervals (t). A mass balance of 80% is generally acceptable for an approximation of P_{app} (Hubatsch et al., 2007). Typical mass balance was found to be between 86% and 109%, thus in the authors opinion provide valid estimations of membrane permeability.

In order to establish the mechanistic nature of absorption for the phenolic acids, the efflux ratio for permeability was calculated as,

DMD Fast Forward. Published on November 17, 2011 as DOI: 10.1124/dmd.111.041665
This article has not been copyedited and formatted. The final version may differ from this version.

$$\text{Efflux ratio} = \frac{P_{app}\ B \rightarrow A}{P_{app}\ A \rightarrow B} \qquad \textit{(eq. 3)}$$

where P_{app} B→A was the permeability coefficient determined by the transport of compound from the basal to the apical compartment, and P_{app} A→B was the permeation coefficient for transport in the apical to basal direction. An efflux ratio = 1 was indicative of passive diffusion, values below 0.5 and above 2 were regarded as indicative of active influx and active efflux respectively.

The residual error, defined as the variation between the observed P_{app} and P_{app}^{trans} in the logarithmic form was calculated as,

$$\text{Residual Error} = \text{Log } P_{app} - \text{Log } P_{app}^{trans} \qquad \textit{(eq. 4)}$$

where a positive residual indicated a greater permeability than predicted and a negative residual indicates a lower permeability.

Data modeling of the training set was performed using the statistical package R (R Development Core Team, 2010). Linear regression and correlation relationships were investigated by analysis of the coefficient of determination (R^2) and Pearson's correlation coefficient respectively. Statistical difference between samples under different cell transport conditions was investigated by analysis of variance, followed by a pairwise multiple comparison test to compare all conditions. Assumption of normality of the data sets and equality of variance was confirmed by Shapiro-Wilk and Levene's test statistics respectively and statistical significance was set at the 0.05 level (PASW statistics. 17). When an experimental Log *D* values could not be located, an *in silico* value was calculated using MarvinSketch, (2010); version 5.3.1, ChemAxon (http://www.chemaxon.com).

DMD Fast Forward. Published on November 17, 2011 as DOI: 10.1124/dmd.111.041665
This article has not been copyedited and formatted. The final version may differ from this version.

Results

The training set

The training set consisted of 30 compounds permeating mainly by the transcellular route and example compounds are shown in Fig. 1. The physicochemical descriptors, summarized in Table 1, are an expanded set based on the works of (Artursson and Karlsson, 1991) and (Camenisch et al., 1998). The compounds have a diversity of structure, a MW range of 146- 631 Da and had a sufficient scope of lipophilicity to permit statistically relevant assessments of MW and Log *D* correlations with Caco-2 permeability.

Inter-laboratory variability

It was our intention to develop a theoretical permeability equation based on a previously reported model (Camenisch et al., 1998) to calculate transport characteristics of the phenolic acids, which were examined in our laboratory using a Caco-2 cell system. Thus, it was necessary to investigate the inter-laboratory reproducibility of the P_{app} and Log *D* physicochemical parameters. Experimental determinations of P_{app} (Fig. 2a) and measurements of 1-octanol/ water distribution coefficients (Fig. 2b) in the current study are in excellent agreement with the published data; results indicated coefficients of determination of $R^2 = 0.96$ and $R^2 = 0.99$ supported by a Pearson's coefficient = 0.99, which was significant at the 1% level.

Training the theoretical transcellular permeability model

Data previously published suggested that, for a given narrow range of molecular weights, Caco-2 permeability was reasonably well explained by a combination of Log *D* and molecular weight with a sigmoidal relationship (Camenisch et al., 1998), referred to as the descriptive absorption model (eq. 5),

$$\text{Log } P_{app}^{trans} = a \bullet \text{Log } D_{oct} - a \bullet \text{Log } (1 + \beta \bullet D_{oct}) + b \qquad \textit{(eq. 5)}$$

where P_{app} was the permeability across the Caco-2 monolayer (cm/s), D_{oct} was the 1-octanol/ water distribution coefficient and a, β and b are model parameters determined by a least squares fit of model (eq. 5) to an experimental data set. In this current study, model (eq. 5) has been expanded so that the model parameters depend on the molecular weight via a quadratic relationship. The choice of a quadratic relationship was driven by inspection of the model parameters obtained by fitting model (eq. 5) to subsets of the training data with different ranges of molecular weights. In brief, the permeability-lipophilicity relationship of the 11 lowest MW drugs (146- 259 Da) in the training set (Table 1), was statistically analyzed by a least-squares non-linear

DMD Fast Forward. Published on November 17, 2011 as DOI: 10.1124/dmd.111.041665
This article has not been copyedited and formatted. The final version may differ from this version.

regression fit of model (eq. 5) to that data subset, giving estimated model parameters a, β and b specific to this range of MW. Subsequently the lowest MW compound was removed and, in exchange, the 12th (262 Da) lowest MW drug was substituted and new model parameters estimated. This process continued until the 11 largest MW drugs (331-631 Da) were used. Thus, a series of model parameters were calculated to describe the change in the relationship between permeability and D_{oct} as MW increased. Each parameter was plotted against the corresponding mean MW for that data subset, showing a quadratic relationship in each case. We therefore generated an expanded set of model parameters incorporating a quadratic dependence on MW. The new parameters were incorporated into the model (eq. 5) to form the theoretical transcellular permeability (TTP) model (eq. 6),

$$\text{Log } P_{app}^{trans} = a' \bullet \text{Log } D_{oct} - a' \bullet \text{Log } (1 + \beta' \bullet D_{oct}) + b' \qquad \textit{(eq.6)}$$

where P_{app}^{trans} was the predicted transcellular permeability, and the expanded model parameters are $a' = (a_0 + (a_1 \bullet MW) + (a_2 \bullet MW^2)$, $\beta' = (\beta_0 + (\beta_1 \bullet MW) + (\beta_2 \bullet MW^2)$, $b' = (b_0 + (b_1 \bullet MW) + (b_2 \bullet MW^2)$ as summarized in Table 2.

Due to the integrated MW function in the TTP model it was possible for the first time to calculate a predicted value for the transcellular permeability of each compound in the training set based on its specific MW and Log D. The TTP model successfully predicted the Caco-2 transcellular permeability of 30 training set compounds as concluded by an excellent agreement between P_{app} and P_{app}^{trans} which was supported by a Pearson's coefficient = 0.96, significant at the 1% level, Fig. 3. The calculated residual errors were between 0.3 to -0.3 log units, except for morphine and sulpiride (-0.4 and -0.5 log units respectively). Furthermore, the residual errors were normally distributed, as concluded by the Shapiro-Wilk test of normality ($p > 0.05$) and residual errors showed no obvious association with MW or Log D (supplemental figure 1).

Shape and MW dependence

A graphical representation of the TTP model was shown in Fig. 4, the 30 training set compounds were arranged in groups of increasing molecular weight and are intersected by contours, which represent the calculated transcellular permeability at specified MW bands. The results indicated, as expected, that a bilinear relationship between permeability and Log D can explain the absorption behaviour of the training set compounds. An increase in MW was associated with a gradual shift towards lower permeability due to weight related restriction of membrane diffusion.

DMD Fast Forward. Published on November 17, 2011 as DOI: 10.1124/dmd.111.041665
This article has not been copyedited and formatted. The final version may differ from this version.

Model evaluation and validation

The results (Table 3) demonstrate that the TTP model can be used to accurately predict the permeability of compounds transported via transcellular passive diffusion with an error between 0.3 to -0.3 log units. A graphical representation (Fig. 5) showed that the P_{app} values of all 9 transcellular compounds fit within the range of permeability predicted by their Log *D* and MW. Investigation of the permeation behaviour of paracellular, active influx or active efflux substrates (Table 3) confirmed that deviation from the predicted model may be explained by a non-transcellular component of uptake across the Caco-2 monolayer. Compounds with a paracellular or active component of uptake resulted in a greater P_{app} value than predicted by the TTP model, indicated by a positive residual error greater than 0.3 log units. An active efflux component resulted in a lower P_{app} value than predicted, indicated by a negative residual error less than -0.3 log units. The model did not predict the active uptake of L-dopa, which may have been complicated by involvement of multiple carrier mediated processes.

Theoretical transcellular permeability for test phenolic acids

To investigate the absorption characteristics of the test phenolic acids, their P_{app}^{trans} values were calculated (Table 4) and compared to the P_{app} values determined in this current study. The results, graphically displayed in Fig. 6, indicated that the TTP model correctly predicted the Caco-2 permeability of 3,4-dimethoxycinnamic acid and ferulic acid. In contrast, the P_{app} values for 5-*O*-CQA and 5-*O*-FQA were greater than predicted by the model. The permeation of caffeic acid and 3,5-diCQA across the Caco-2 membrane were found to be slightly less than predicted by the model.

Mechanistic investigation of phenolic acid absorption

The relevance of the TTP model for the estimation of absorption pathways was investigated using Caco-2 mechanistic studies to elucidate the involvement of paracellular, active efflux and active uptake components of transport. The results summarized in Table 4 and Fig. 7 revealed that bi-directional transport was linear with respect to time and concentration with a corresponding efflux ratio approaching 1 for all tested phenolic acids, except 3,5-diCQA. Investigation of the route of absorption was deduced by varying the diameter of the tight junction pore, as measured by TEER resistance to permeation. Ferulic acid was the only test compound with no statistical difference between the P_{app} value at a TEER of 1155 ±70 $\Omega \cdot cm^2$ and transport at low TEER (680 ±40 $\Omega \cdot cm^2$) and thus we concluded that ferulic acid transport was mainly passive transcellular. In contrast, the P_{app} values for 5-*O*-CQA and 5-*O*-FQA were significantly ($p < 0.05$) higher at low TEER. Caffeic acid was previously shown to be permeated mainly via the paracellular pathway (Konishi and Kobayashi, 2004). Thus, no

DMD Fast Forward. Published on November 17, 2011 as DOI: 10.1124/dmd.111.041665
This article has not been copyedited and formatted. The final version may differ from this version.

further mechanistic investigations were performed in this current study for this test compound. Finally, the transport of 3,5-diCQA was more complex; mechanistic studies revealed involvement of an active efflux component, as concluded by an efflux ratio of 5.4.

Efflux of 3,5-diCQA was further investigated using inhibitors which have been shown previously to inhibit ABC transport proteins (Matsson et al., 2009). The results of the current study (Table 5) suggest that all inhibitors significantly ($p < 0.05$) reduced the B→A permeation (efflux) of 3,5-diCQA. Pairwise analysis of the statistical difference between mean P_{app} values within the inhibitor group confirmed there was no significant difference between the potency of MK 571, cyclosporine A and apigenin. However, the potency of quercetin was significantly ($p < 0.05$) greater than the other 3 inhibitors. These results suggest that ABC transport proteins are involved in the active efflux of 3,5-diCQA in a serosal to luminal direction and the process may occur by a combination of BCRP, P-gp and MRP2 proteins.

DMD Fast Forward. Published on November 17, 2011 as DOI: 10.1124/dmd.111.041665
This article has not been copyedited and formatted. The final version may differ from this version.

Discussion

For the first time the absorption characteristics of a series of dietary phenolic acids were investigated using a theoretical permeability model. Lipophilicity is considered as an important determinant for absorption (van de Waterbeemd, 2009) and is commonly measured as the partition coefficient (log *P*) in an 1-octanol/aqueous system (van de Waterbeemd and Gifford, 2003). The relevance of Log *P* to membrane permeability has been attributed to the ability of hydrated 1-octanol to simulate the structural homology and hydrogen bonding capacity of more complex lipid bilayers (Artursson et al., 2001). Furthermore, the distribution coefficient (Log *D*) can be considered to provide a more meaningful description of partition processes in the body for ionisable compounds (van de Waterbeemd and Gifford, 2003) and encodes several physicochemical properties: hydrogen bonding capacity, influence of ionization on solubility and molecular weight (Liu et al., 2011;van de Waterbeemd, 1998). A good predictive relationship between P_{app} and Log *D,* with a molecular weight as a third descriptor, has been observed in the Caco-2 model (Camenisch et al., 1998). Thus, the previously reported descriptive absorption model (eq. 5) based on a bilinear relationship between P_{app} and Log *D* was thought to be suitable for further investigation of absorption across Caco-2 cell monolayers.

Statistical modeling performed on the training set revealed a quadratic relationship between the model parameters and MW. When these novel expanded parameters were integrated into the new TTP model (eq. 6), a more useful relationship between P_{app} and Log *D* could be obtained compared to the descriptive absorption model (eq. 5), which was only fitted by spline-smoothing to create a model limited to the estimation of passive diffusion (Camenisch et al., 1998). An excellent fit was observed between the TTP model and training set data ($R^2 = 0.93$). A bilinear relationship between permeability and lipophilicity was described with MW dependence due to membrane partitioning and diffusion effects (Xiang and Anderson, 1994). The transport plateau often observed with very lipophilic compounds (high Log *D*) is due to rate limiting diffusion of lipophilic compounds through the stagnant aqueous boundary layer close to the membrane surface (Stehle and Higuchi, 1972).

A MW dependence for permeability was observed in the TTP model (eq. 6) as indicated by the positioning of the predicted permeation curves (Fig. 4), which show a reduction in permeability as MW increases as was previously reported (Camenisch et al., 1998). The importance of MW in membrane permeability can be attributed to a role in lipophilicity as described by equation 7 (van de Waterbeemd, 1998),

$$\text{Log } D = aV - \Lambda \qquad \textit{(eq. 7)}$$

where Log *D* was the distribution coefficient, *a* was a regression constant, *V* was the molar volume (molecular size component), and Λ was a polarity term (related to hydrogen bonding capacity). Thus, the affinity of a compound for a lipophilic environment can be considered as a product of its molecular size and hydrogen bonding capacity. Furthermore, molecular size was shown to be inversely related to the diffusion coefficient *D* as revealed by the Einstein-Stokes equation. Thus molecular size, represented by MW in this study may be considered as a governing factor for transcellular diffusion in biological membranes (Xiang and Anderson, 1994).

Using the TTP model, good estimations of the transcellular permeability of 9 structurally diverse compounds in the validation set were obtained with a Pearson's correlation coefficient = 0.97, significant at the 1% level. The scope of the TTP model to estimate transport mechanisms of absorption was evaluated using commonly used markers of paracellular, active influx and active efflux processes in the Caco-2 model. The results suggested that deviation from the model may be used to reveal interference by non-transcellular transport processes, however additional transport studies are required to indicate which mechanisms have a role. Divergences can be rationalized by considering the design of the TTP model, which predicts only the transcellular fraction of absorption, thus any transport via the paracellular route would be observed as an additional flux. Similarly, any active transport would enhance (influx) or hinder (efflux) permeability and result in a positive or negative deviation from the theoretical value respectively. To distinguish between paracellular and active processes we recommend that an additional Caco-2 mechanistic study be performed. Transport of the test compound under conditions of variable TEER has become a common method to elucidate the role of tight junctions in membrane permeation (Konishi and Kobayashi 2004). Compounds transported primarily via the paracellular route will be attenuated at high TEER if the pore size was sufficiently restrictive. Alternatively, transport of the test compound under chilled conditions (on ice) would retard active uptake, thus revealing the involvement of active processes.

Interestingly, the model over-estimated the permeability of L-dopa. The poor uptake may be explained by differential expression of the amino acid transporter (Sun et al., 2002) in Caco-2 cells or the involvement of active efflux as suggested by others (Fraga & Soares-da-Silva 2006). In reference to human bioavailability, comparative *in vivo*/ Caco-2 *in vitro* permeability relationships have been previously characterized (Sun et al., 2002). It should be noted that a good correlation exists between Caco-2 permeability and human intestinal uptake. However, the predicted permeability for carrier mediated or metabolized compounds by the Caco-2

DMD Fast Forward. Published on November 17, 2011 as DOI: 10.1124/dmd.111.041665
This article has not been copyedited and formatted. The final version may differ from this version.

model may be expected to differ from *in vivo* due to significant differences in gene expression of specific transporters and metabolic enzymes (Sun et al., 2002).

The permeability of the phenolic acids has never been investigated using a theoretical permeability model before and the results of this study represent valuable information that can streamline future polyphenol bioavailability investigations. Using the TTP model we have calculated the theoretical transcellular permeability of 6 phenolic acids based on their MW and our experimentally determined Log *D* values. Mechanistic studies were performed on Caco-2 monolayers to evaluate the accuracy of the TTP model when estimating the contribution of specific pathways in phenolic acid absorption (Table 4) and are discussed below.

In the current study, the efflux ratio of ferulic acid was equivalent to 1, suggesting transport was passive and permeation was independent of tight junction integrity, thus we concluded that the model correctly identified the absorption as passive transcellular transfer, which was in agreement which previous investigations (Poquet et al., 2008). We infer that the transport of 3,4-dimethoxycinnamic acid was also passive transcellular, but no mechanistic data was available at this time. The transport of 5-*O*-CQA and 5-*O*-FQA was found to be linear with respect to time and concentration, bi-directional permeation was equivalent to 1 and transport was significantly increased ($p < 0.05$) at low TEER. Thus we concluded that the transport of these compounds was passive paracellular, as correctly predicted by the TTP model. The P_{app} value for 3,5-diCQA was less than predicted, as concluded by a residual error less than -0.3 log units, suggesting transport was impeded by active efflux or cell metabolism. De-esterification was not thought to be a major factor in the absorption characteristics of 3,5-diCQA as concluded by the observation that 3,5-diCQA was a poor substrate for chlorogenate esterase (Guy et al., 2009). The relative resistance of the diCQAs to hydrolysis and negligible metabolism was apparent in the current study as shown by an excellent mass balance recovery of 98 ±3%. Furthermore, mechanistic studies revealed that permeation was enhanced in the B→ A direction, efflux ratio of 5.4, thus the involvement of an active efflux transporter was confirmed. Further efflux inhibition studies have implicated the ABC transporter family as important to the secretion of 3,5-diCQA in the serosal to lumenal direction. This compound was the most lipophilic HCA investigated and it is likely to partition readily in to the lipid bilayer and diffuse via the lipid envelope, suggesting that partitioned compound would be ideally placed for rapid export to the lumen by P-gp, BCRP and MRP2 which are co-localized to the apical membrane of intestinal epithelial cells and have notable affinity for lipophilic substrates (Matsson et al., 2009).

The transport behaviour of caffeic acid was estimated to be a substrate for efflux or extensive metabolism. We have previously reported that the Caco-2 metabolism of caffeic acid accounts for approximately 0.1% of the

amount absorbed (Farrell et al., 2011), thus extensive metabolism was ruled out as a reason for the reduced permeation. Investigation of the bi-directional transport of caffeic acid revealed that transport was passive as concluded by the efflux ratio of 1.2. A possible explanation for this discrepancy may be attributed to small losses due to membrane binding because the mean mass balance for the transport study was 84%.

In conclusion a refined theoretical model has been used to successfully predict the transcellular permeability of an external validation set, and a good estimation of the major transport pathways was observed. The usefulness of theoretical models to predict Caco-2 permeability could be a benefit to *in vitro* absorption studies and may be of interest to human bioavailability studies since permeability coefficients for passive transcellular transport in Caco-2 cells are good indicators of oral absorption (Sun et al., 2002;Press and Grandi, 2008).

Acknowledgements

We would like to thank D. Barron (Nestlé Research Center, Switzerland) for his generous gift of the feruloylquinic acid standard.

Authorship Contributions

Participated in research design: Farrell, Poquet, Barber, Williamson.

Conducted experiments: Farrell, Barber

Contributed new reagents or analytical tools: Barber, Dew

Performed data analysis: Farrell, Barber

Contributed to the writing of the manuscript: Farrell, Poquet, Barber, Williamson,

Reference

Alsenz J, and Haenel E (2003) Development of a 7-day, 96-well Caco-2 permeability assay with high-throughput direct UV compound analysis. *Pharm Res* **20:** 1961-1969.

Artursson P, and Karlsson J (1991) Correlation between oral-drug absorption in humans and apparent drug permeability coefficients in human intestinal epithelial (Caco-2) cells. *Biochem Biophys Res Commun* **175:** 880-885.

Artursson P, Palm K, and Luthman K (2001) Caco-2 monolayers in experimental and theoretical predictions of drug transport. *Adv Drug Deliv Rev* **46:** 27-43.

Avdeef A, and Tam KY (2010) How well can the Caco-2/Madin-Darby canine kidney models predict effective human jejunal permeability? *J Med Chem* **53:** 3566-3584.

Bernards CM, and Hill HF (1992) Physical and chemical-properties of drug molecules governing their diffusion through the spinal meninges. *Anesthesiol* **77:** 750-756.

Camenisch G, Alsenz J, van de Waterbeemd H, and Folkers G (1998) Estimation of permeability by passive diffusion through Caco-2 cell monolayers using the drugs' lipophilicity and molecular weight. *Eur J Pharm Sci* **6:** 313-319.

Farrell T, Poquet P, Dionisi F, Barron D, and Williamson G (2011) Characterization of hydroxycinnamic acid glucuronide and sulfate conjugates by HPLC–DAD–MS2: Enhancing chromatographic quantification and application in Caco-2 cell metabolism. *J Pharm Biomed Anal* **55:** 1245-1254.

Fraga S & Soares-da-Silva P (2006) P-glycoprotein and multidrug resistance-associated protein (MRP) reverse the intestinal transport of L-DOPA, a LAT2 substrate. *FASEB J* **20:** (5) A841.

Garberg P, Ball M, Borg N, Cecchelli R, Fenart L, Hurst RD, Lindmark T, Mabondzo A, Nilsson JE, Raub TJ, Stanimirovic D, Terasaki T, Oberg JO, and Osterberg T (2005) In vitro models for the blood-brain barrier. *Toxicol In Vitro* **19:** 299-334.

Gramatte T, Oertel R, Terhaag B, & Kirch W (1996) Direct demonstration of small intestinal secretion and site-dependent absorption of the beta-blocker talinolol in humans. *Clin Pharmacol Ther* **59:** (5) 541-549.

Guy PA, Renouf M, Barron D, Cavin C, Dionis F, Kochhar S, Rezzi S, Williamson G, & Steiling H (2009) Quantitative analysis of plasma caffeic and ferulic acid equivalents by liquid chromatography tandem mass spectrometry. *J Chromatogr B-Analyt Technol Biomed and Life Sci* **877:** (31) 3965-3974

Henry-Vitrac C, Ibarra A, Roller M, Merillon JM, and Vitrac X (2010) Contribution of chlorogenic acids to the inhibition of human hepatic glucose-6-phosphatase activity in vitro by svetol, a standardized decaffeinated green coffee extract. *J Agric Food Chem* **58:** 4141-4144.

Hilgendorf C, Spahn-Langguth H, Regardh CG, Lipka E, Amidon GL, and Langguth P (2000) Caco-2 versus Caco-2/HT29-MTX co-cultured cell lines: Permeabilities via diffusion, inside- and outside-directed carrier-mediated transport. *J Pharm Sci* **89:** 63-75.

Hosoya K, Yamamoto A, Akanuma S, & Tachikawa M (2010) Lipophilicity and transporter influence on blood-retinal barrier permeability: a comparison with blood-brain barrier permeability. *Pharma Res* **27**: (12) 2715-2724.

Hubatsch I, Ragnarsson EGE, and Artursson P (2007) Determination of drug permeability and prediction of drug absorption in Caco-2 monolayers. *Nat Protoc* **2:** 2111-2119.

Kern C, and Bernards CM (1997) Ascorbic acid inhibits spinal meningeal catechol-o-methyl transferase in vitro, markedly increasing epinephrine bioavailability. *Anesthesiol* **86:** 405-409.

Konishi Y, and Kobayashi S (2004) Transepithelial transport of chlorogenic acid, caffeic acid, and their colonic metabolites in intestinal caco-2 cell monolayers. *J. Agric Food Chem.* **52:** 2518-2526.

Lennernas H, Palm K, Fagerholm U, and Artursson P (1996) Comparison between active and passive drug transport in human intestinal epithelial (Caco-2) cells in vitro and human jejunum in vivo. *Int J Pharm* **127:** 103-107.

Liu XL, Testa B, and Fahr A (2011) Lipophilicity and its relationship with passive drug permeation. *Pharm Res* **28:** 962-977.

Matsson P, Pedersen JM, Norinder U, Bergstrom CAS, and Artursson P (2009) Identification of novel specific and general inhibitors of the three major human ATP-binding cassette transporters P-gp, BCRP and MRP2 among registered drugs. *Pharm Res* **26:** 1816-1831.

Mazzobre MF, Roman MV, Mourelle AF, and Corti HR (2005) Octanol-water partition coefficient of glucose, sucrose, and trehalose. *Carbohydr Res* **340:** 1207-1211.

Obata K, Sugano K, Saitoh R, Higashida A, Nabuchi Y, Machida M, and Aso Y (2005) Prediction of oral drug absorption in humans by theoretical passive absorption model. *Int J Pharm* **293:** 183-192.

Palm K, Stenberg P, Luthman K, and Artursson P (1997) Polar molecular surface properties predict the intestinal absorption of drugs in humans. *Pharm Res* **14:** 568-571.

Poquet L, Clifford MN, and Williamson G (2008) Transport and metabolism of ferulic acid through the colonic epithelium. *Drug Metab Dispos* **36:** 190-197.

Press B, & Di Grandi D (2008) Permeability for intestinal absorption: Caco-2 assay and related issues. *Curr Drug Metab* **9:** (9) 893-900.

Shen Q, Lin YL, Handa T, Doi M, Sugie M, Wakayama K, Okada N, Fujita T, & Yamamoto A (2006) Modulation of intestinal P-glycoprotein function by polyethylene glycols and their derivatives by in vitro transport and in situ absorption studies. *Int J Pharm* **313:** (1-2) 49-56.

Shirasaka Y, Li Y, Shibue Y, Kuraoka E, Spahn-Langguth H, Kato Y, Langguth P, & Tamai I (2009). Concentration-dependent effect of naringin on intestinal absorption of beta(1)-adrenoceptor antagonist talinolol mediated by P-glycoprotein and organic anion transporting polypeptide (OATP). *Pharma Res* **26:** (3) 560-567.

Stehle RG, and Higuchi WI (1972) In-vitro model for transport of solutes in 3 phase system .1. Theoretical principles. *J Pharm Sci* **61:** 1922-1930.

Stein PC, di Cagno M, & Bauer-Brandl A (2011) A novel method for the investigation of liquid/liquid distribution coefficients and interface permeabilities applied to the water-octanol-drug system. *Pharma Res* **28:** (9) 2140-2146.

Sugano K, Kansy M, Artursson P, Avdeef A, Bendels S, Di L, Ecker GF, Faller B, Fischer H, Gerebtzoff G, Lennernaes H, and Senner F (2010) Coexistence of passive and carrier-mediated processes in drug transport. *Nat Rev Drug Discov* **9:** 597-614.

Sun DX, Lennernas H, Welage LS, Barnett JL, Landowski CP, Foster D, Fleisher D, Lee KD, & Amidon GL (2002) Comparison of human duodenum and Caco-2 gene expression profiles for 12,000 gene sequences tags and correlation with permeability of 26 drugs. *Pharm Res* **19:** (10) 1400-1416.

Troutman MD & Thakker DR (2003) Rhodamine 123 requires carrier-mediated influx for its activity as a P-glycoprotein substrate in Caco-2 cells. *Pharma Res* **20:** (8) 1192-1199.

van Dam RM, and Hu FB (2005) Coffee consumption and risk of type 2 diabetes - A systematic review. *JAMA* **294:** 97-104.

van de Waterbeemd H (1998) The fundamental variables of the biopharmaceutics classification system (BCS): A commentary. *Eur J Pharm Sci* **7:** 1-3.

van de Waterbeemd H (2009) Improving compound quality through in vitro and in silico physicochemical profiling. *Chem Biodivers* **6:** 1760-1766.

van de Waterbeemd H, and Gifford E (2003) ADMET in silico modelling: Towards prediction paradise? 104. *Nat Rev Drug Discov* **2:** 192-204.

Wang Z, Clifford MN, and Sharp P (2008) Analysis of chlorogenic acids in beverages prepared from Chinese health foods and investigation, in vitro, of effects on glucose absorption in cultured Caco-2 cells. *Food Chem* **108:** 369-373.

Xiang TX, and Anderson BD (1994) The relationship between permeant size and permeability in lipid bilayer-membranes. *J Membr Biol* **140:** 111-122.

Yamashita S, Furubayashi T, Kataoka M, Sakane T, Sezaki H, and Tokuda H (2000) Optimized conditions for prediction of intestinal drug permeability using Caco-2 cells. *Eur J Pharm Sci* **10:** 195-204.

Yazdanian M, Glynn SL, Wright JL, and Hawi A (1998) Correlating partitioning and Caco-2 cell permeability of structurally diverse small molecular weight compounds. *Pharm Res* **15:** 1490-1494.

Footnote

This research was supported by Nestlé Research Center, Switzerland.

DMD Fast Forward. Published on November 17, 2011 as DOI: 10.1124/dmd.111.041665
This article has not been copyedited and formatted. The final version may differ from this version.

Legends for Figures

Fig.1. Example compounds investigated in the current study.

Fig.2. A: Comparison of apparent permeability coefficients determined experimentally ($LogP_{app}^{exp}$) in differentiated Caco-2 monolayers (n = 3) with data previously published for the training set compounds (Artursson and Karlsson, 1991). B: Comparison of experimentally determined 1-octanol/ water distribution coefficients (Log D^{exp}) at 37 °C, pH 7.4 by the shake flask method (n = 10) with published measurements. (●): mean of the experimentally determined value ±S.D.

Fig.3. Relationship between apparent permeability (Log P_{app}) and predicted transcellular permeability ($LogP_{app}^{trans}$) of training set compounds as predicted by the TTP model (eq. 6).

Fig.4. Comparison of the apparent permeability for the training set compounds and the predictions for transcellular permeability based on the Log *D* and molecular weight (MW). Training set compounds: ▲: 146-194 Da; ○ 231- 346 Da; ● 360- 496 Da; ■ 555 Da and □ 631 Da. Dashed line: calculated transcellular permeability predictions for given MW values.

Fig.5. Graphical representation of the fit for 9 non-training set compounds transported by the transcellular route. Inset: good linearity ($R^2 = 0.86$) between apparent permeability ($LogP_{app}$) and the predicted transcellular permeability ($LogP_{app}^{trans}$) calculated using the TTP model. Dashed line: calculated transcellular permeability predictions for given MW values. (1): acetylsalicylic acid, MW 180. (2) salicylic acid, MW 138. (3): caffeine, MW 194. (4): aminopyrine, MW (231). (5): fluvastatin, MW 411. (6): nevirapine, MW 266. (7): carbamazepine, MW 236. (8): griseofulvin, MW 353. (9): naproxen, MW 230.

Fig.6. Comparison of the apparent permeability of 6 phenolic acids determined in the current study and the predicted transcellular permeability calculated using the TTP model. Values are mean $LogP_{app}$ ± S.D. Dashed lines: calculated transcellular permeability predictions. Inset: comparison of the apparent permeability (○) and the predicted transcellular permeability ± 0.3 Log units (residual error) (●). (1): 5-*O*-CQA; (2): 5-*O*-FQA; (3): caffeic acid; (4): 3,5-diCQA; (5): ferulic acid; (6): 3,4-dimethoxycinnamic acid.

Fig.7. Time and concentration dependent permeation of (A,B): 5-*O*-CQA; (C,D): 5-*O*-FQA; (E,F): 3,5-diCQA. Solid line: linear relationship (R^2 greater than 0.85). Dashed line: non-linear relationship. (○): apical to basal permeation. (●) basal to apical permeation.

DMD Fast Forward. Published on November 17, 2011 as DOI: 10.1124/dmd.111.041665
This article has not been copyedited and formatted. The final version may differ from this version.

Table 1

Table 1. Physicochemical properties and Caco-2 monolayer permeability of training set compounds.

	Compound	Molecular weight	Distribution coefficient (Log *D*)[a]	Caco-2 permeability ($LogP_{app}$)[b]
	Training Set			
1	Coumarin	146	1.39	-4.11
2	Theophylline	180	-0.02	-4.35
3	Epinephrine	183	-2.59	-6.02
4	Antipyrine	188	0.56[d]	-4.36[f]
5	Guanoxan	194	-0.83	-4.71
6	Guanabenz	231	1.67	-4.14
7	Lidocaine	234	1.63	-4.21
8	Alprenolol	249	1.00/ 1.08[c]	-4.39/ -4.43[c]
9	Phenytoin	252	2.50[f]	-4.39[f]
10	Ketoprofen	254	0.47[g]/ 0.19[h]	-4.63[e]
11	propranolol	259	1.54	-4.38
12	Tiacrilast	262	-1.05	-4.90
13	Practolol	266	-1.40	-5.86
14	Metoprolol	267	0.07/ -0.24[c]	-4.57/ -4.55[c]
15	Imipramine	280	2.52	-4.26
16	Diazepam	285	2.10[f]	-4.39[f]
17	Morphine	285	-0.44[f]	-5.08[f]
18	Testosterone	288	3.31	-4.23
19	Warfarin	308	0.90	-4.27
20	Piroxicam	331	0.00	-4.33[e]
21	Sulpiride	342	-1.15	-6.16

DMD Fast Forward. Published on November 17, 2011 as DOI: 10.1124/dmd.111.041665
This article has not been copyedited and formatted. The final version may differ from this version.

22	Corticosterone	346	1.89	-4.26
23	Nitrendipine	360	0.97	-4.77
24	Hydrocortisone	362	1.53/ 1.55[c]	-4.67/ -4.78[c]
25	Felodipine	384	3.48	-4.64
26	Dexamethasone	392	1.74	-4.90
27	Verapamil	455	3.40	-4.80
28	Mibefradil	496	3.66	-4.87
29	Ceftriaxone	555	-1.23	-6.88
30	Remikiren	631	2.75	-6.13
	n = 30			

a: 1-octanol/ water (pH 7.4) distribution coefficient taken from Artursson and Karlsson (1991); Camenisch et al. (1998). b: permeability in differentiated Caco-2 monolayers, taken from Camenisch et al. (1998). Experimental data from c: current study; d: Avdeef and Tam. (2010); e: Hilgendorf et al. (2000); f: Garberg et al. (2005); g: calculated Log *D* from MarvinSketch (2010); h: experimental Log *D* from Stein et al. (2011). Note: the calculated Log *D* value of ketoprofen was used in the current study because an experimental Log *D* value based on 1-octantol/ water was not available at the time.

Table 2

Table 2. Summary of model parameters for the theoretical transcellular permeability (TTP) model with integrated molecular weight function.

	Model Parameters				
	$a' = a_0 + (a_1 \cdot MW) + (a_2 \cdot MW^2)$		$\beta' = \beta_0 + (\beta_1 \cdot MW) + (\beta_2 \cdot MW^2)$		$b' = b_0 + (b_1 \cdot MW) + (b_2 \cdot MW^2)$
a_0	0	β_0	0	b_0	-3.18
a_1	4.82×10^{-4}	β_1	0	b_1	-1.25×10^{-2}
a_2	2.35×10^{-5}	β_2	7.73×10^{-5}	b_2	4.89×10^{-5}

Model parameters a', β' and b' are derived by least-squares non-linear regression fit of the descriptive absorption model (eq. 5). MW: molecular weight.

Table 3

Table 3. Comparison of the physicochemical properties, percentage human oral absorption, Caco-2 permeability and predicted transcellular permeability of non-training set compounds.

Compound	MW	Distribution coefficient (Log *D*)	[refs]	Absolute bioavailability %	[refs]	Caco-2 permeability ($LogP_{app}$)	[refs]	Model prediction ($LogP_{app}^{trans}$)	Residual error
Non-Training Set									
Transcellular									
Salicylic acid	138	-1.44	[h]	100	[h, e]	-4.92/ -4.89	[b]/[a]	-4.73	-0.19
Acetylsalicylic acid	180	-2.57/ -2.34	[b]/[a]	100	[h]	-5.62	[b]	-5.84	0.22
Caffeine	194	0.02	[h]	100	[h]	-4.51	[h]	-4.34	-0.17
Naproxen	230	3.3	[i]	100	[e]	-4.05	[d]	-4.30	0.25
Aminopyrine	231	0.63	[h]	100	[h]	-4.44	[h]	-4.34	-0.10
Nevirapine	266	1.81	[h]	>90	[h]	-4.52	[h]	-4.37	-0.15
Carbamazepine	236	2.45	[e]	95	[e]	-4.21	[f]	-4.31	0.11
Griseofulvin	353	2.47	[h]	95	[e]	-4.44	[h]	-4.54	0.11
Fluvastatin	411	1.09	[i]	95	[e]	-4.64	[j]	-4.71	0.07

Paracellular									
Mannitol	182	-3.10	[b]	16	[h]	-5.58	[b]	-6.52	0.94
Active uptake									
Glucose	180	-2.83	[c]	100	[e]	-4.70	[d]	-6.25	1.55
Gly-pro	172	-3.32	[i]	100	[e]	-5.21	[j]	-6.47	1.26
L-Dopa	197	-1.22/-1.38	[k]/[i]	100	[e]	-6.00	[g]	-5.05	-0.95
Active efflux									
Cimetidine	252	-0.4	[g]	60	[e]	-6.48	[g]	-4.63	-1.85
Rhodamine 123	380	0.53	[l]	poor	[o]	-5.79	[l]	-4.65	-1.14
Talinolol	363	1.1	[m]	55	[n]	-6.69	[j]	-4.58	-2.12

Pathway of absorption was based on percentage human oral absorption and mechanistic studies [see refs]. For compounds transported via transcellular diffusion the Caco-2 permeability ($LogP_{app}$) can be estimated by the TTP model prediction with a residual between 0.3 and -0.3.Residual error >0.3: a paracellular or active influx component; <-0.3: an active efflux component. [Refs]: a: experimental data from current study. b: Artursson and Karlsson (1991); Camenisch et al. (1998). c: Mazzobre et al. (2005). d: Lennernas et al. (1996). e: Avdeef and Tam (2010). f: Alsenz and Haenel (2003). g: Garberg et al. (2005). h: Yazdanian et al. (1998). i: MarvinSketch (2010): j: Hilgendorf et al. (2000); k: Hosoya et al. (2010); l: Troutman & Thakker (2003); m: Shirasaka et al. (2009); n: Gramatte et al. (1996); o: Shen et al. (2006).

Table 4

Table 4. Summary of the mechanistic data for permeability of phenolic acids across Caco-2 monolayers & the calculated transcellular permeability predictions

Compound		Mechanistic studies						Evaluation of the Model Prediction		
		Caco-2 permeability		Efflux	Variable TEER resistance					
	Log $D_{pH\ 7.4}$	P_{app} (x 10^{-6}) cm/s		ratio $\frac{P_{app}\ B\rightarrow A}{P_{app}\ A\rightarrow B}$	P_{app} (x 10^{-6}) cm/s		Dominant absorption characteristic	$LogP_{app}$	$LogP_{app}^{trans}$	Residual error
		A→ B	B→ A		High	Low				
Caffeic acid	-1.35	1.4 ±0.1	1.7 ±0.1	1.2	[Konishi and Kobayashi (2004)]		paracellular	-5.84 ±0.1	-5.03	-0.8
5-*O*-CQA	-3.05	0.38 ±0.1	0.33 ±0.1	0.9	0.25 ±0.1	0.77 ±0.1†	paracellular	-6.42 ±0.2	-11	4.6
3,5-diCQA	-1.04	0.14 ±0.02	0.72 ±0.1	5.1	0.05 ±0.01*	0.68 ±0.1†	efflux	-6.85 ±0.1	-6.34	-0.5
Ferulic acid	-1.19	10.0 ±0.2	10.2 ±1.1	1	10.8 ±0.6	11.2 ±0.8	transcellular	-4.98 ±0.1	-5.01	0.03
5-*O*-FQA	-2.79	0.25 ±0.1	0.28 ±0.1	1.1	0.31 ±0.1	1.7 ±0.4†	paracellular	-6.60 ±0.2	-10.6	4

DMCIN	-1.01	19.9 ±0.1	21.7 ±0.7	1.1	n.d.	n.d.	transcellular	-4.7 ±0.003	-4.93	0.2

Permeability in all mechanistic studies was investigated by measuring the transfer of compound (500 μM) from donor (pH 7.4) to receiver (pH 7.4) compartment after 1 h incubation with confluent monolayers (n = 3) at 37 °C in a humidified 5% CO_2 atmosphere. Values are mean apparent permeability coefficient (P_{app}) ± S.D. †: statistical significant difference ($p< 0.05$) between mean experimental Caco-2 permeability (A→B) and permeability at low TEER. *: statistical significant difference ($p< 0.05$) between mean experimental Caco-2 permeability (A→B) and permeability at high TEER. [ ]: data could not be translated from reference, see Konishi and Kobayashi (2004) for details. n.d.: not determined. diCQA; dicaffeoylquinic acid; CQA: caffeoylquinic acid; FQA: feruloylquinic acid; DMCIN: 3,4-dimethoxycinnamic acid.

Table 5

Table 5. Basal to apical permeability (efflux) of 3,5-di-*O*-caffeoylquinic acid in the presence of ABC transporter inhibitors.

Inhibitor	Transporter Affected[a]	Permeability P_{app} B →A cm/s	% Inhibition	Inhibitor Concentration Current Study (μM)
Quercetin	MRP-2, BCRP, P-gp	0.13 ±0.03	65†	25
MK 571	MRP-2	0.21 ±0.04	46†	25
Cyclosporin A	P-gp	0.25 ±0.06	35†	10
Apigenin	BCRP	0.26 ±0.04	32†	25
Control	-	0.39 ±0.03	-	-

Permeability coefficients (P_{app}) in the basal to apical direction (B →A) were determined by analysis of the apical solution after basal incubation (1 h) of 3,5-diCQA (500 μM) with differentiated monolayers (n = 6) and ABC transporter inhibitor (apical side), 37 °C, 5% CO_2. P_{app}: expressed as $x10^{-6}$ ±S.D. % inhibition: [P_{app} control - P_{app} inhibitor]/ P_{app} control × 100. a: inhibitor specificity evaluated by Matsson et al. (2009). †: statistical significant reduction ($p< 0.05$) of 3,5-diCQA efflux compared to control condition.

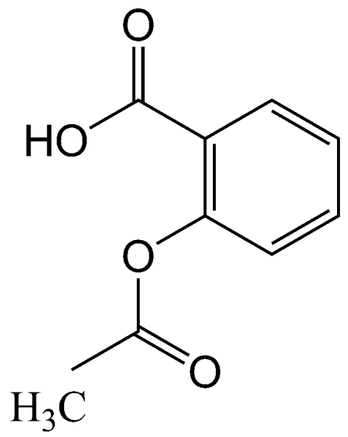

acetylsalicylic acid

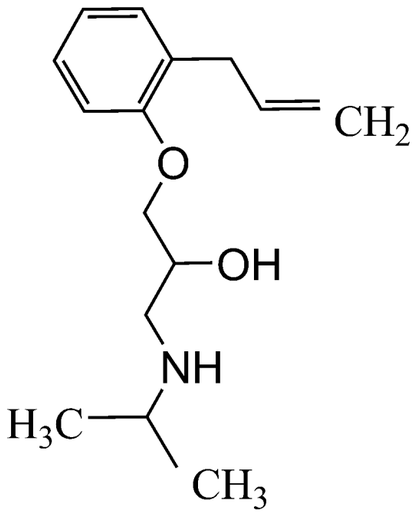

alprenolol

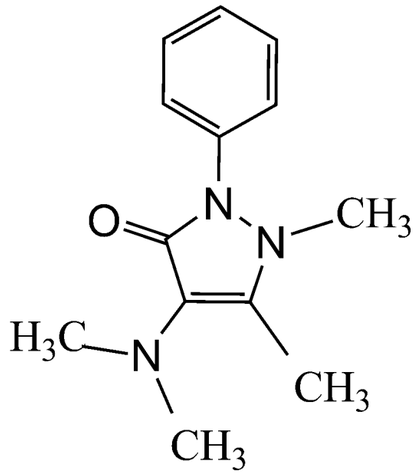

aminopyrine

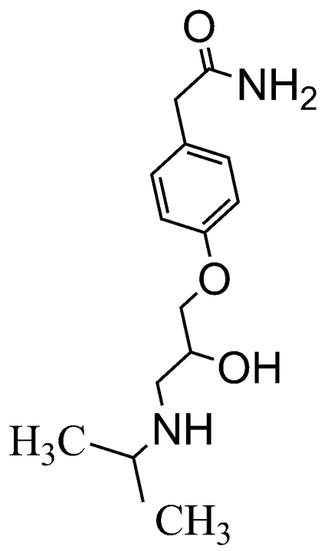

atenolol

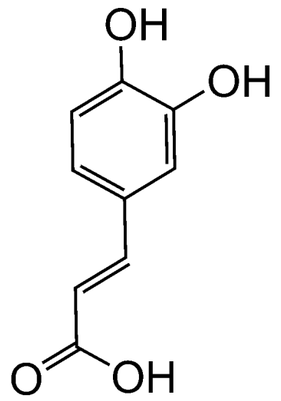

caffeic acid

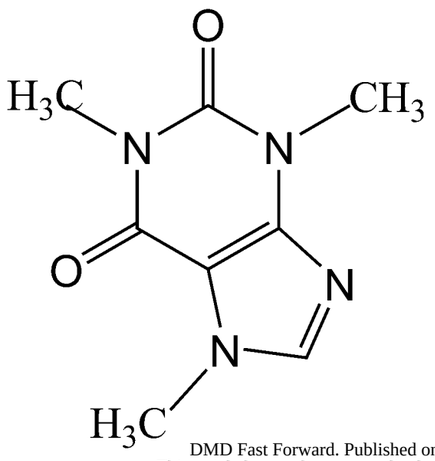

caffeine

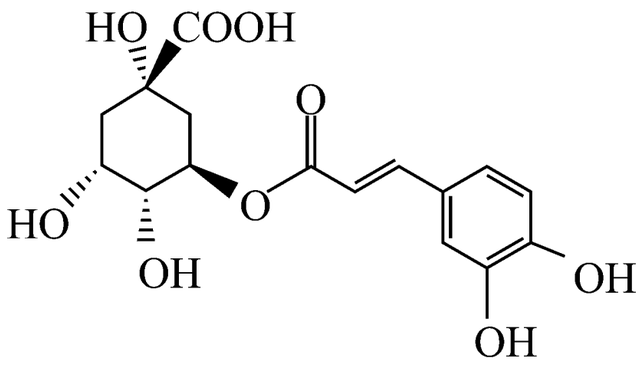

5-*O*-caffeoylquinic acid

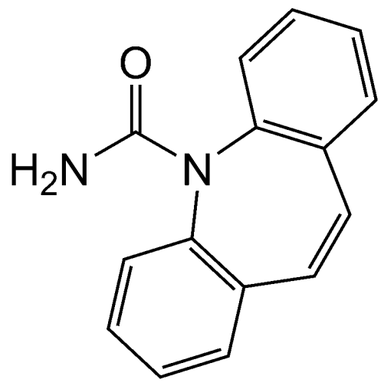

carbamazepine

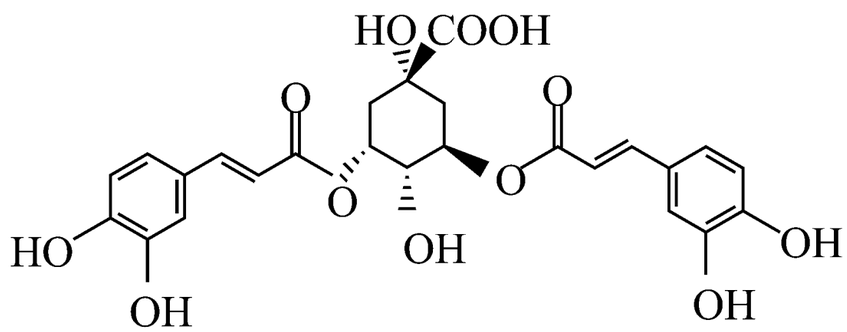

3,5-*O*-dicaffeoylquinic acid

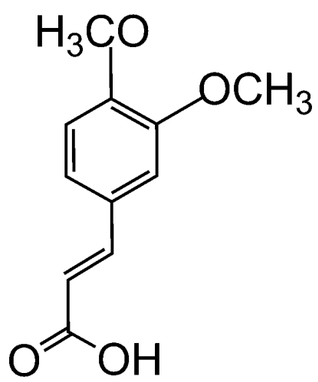

3,4-dimethoxycinnamic acid

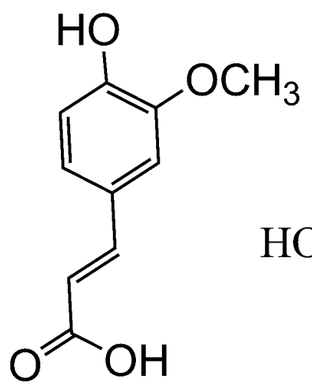

ferulic acid

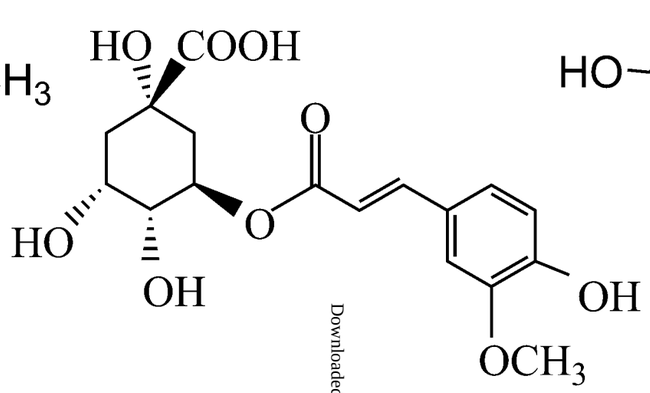

5-*O*-feruloylquinic acid

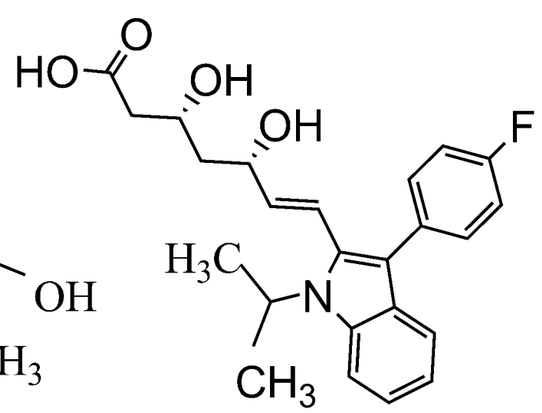

fluvastatin

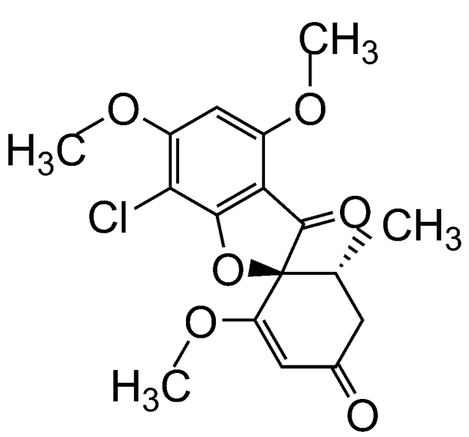

griseofulvin

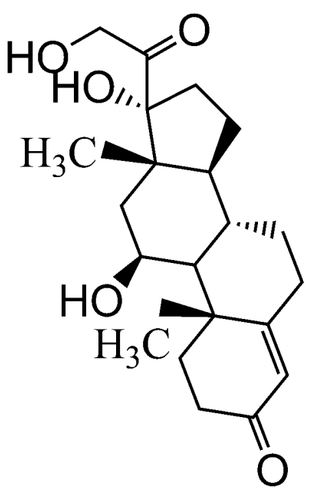

hydrocortisone

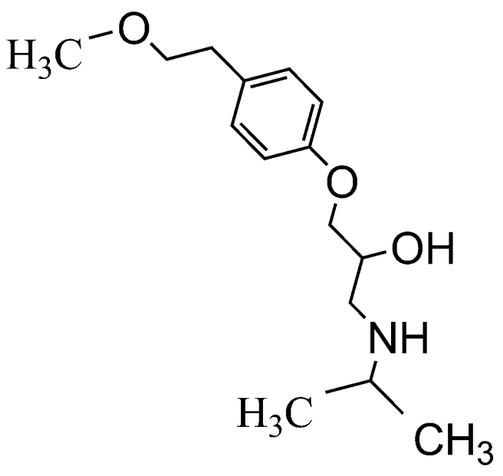

metoprolol

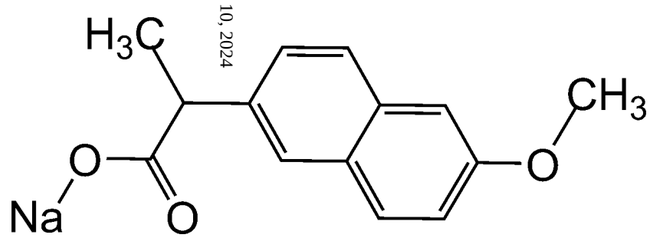

naproxen

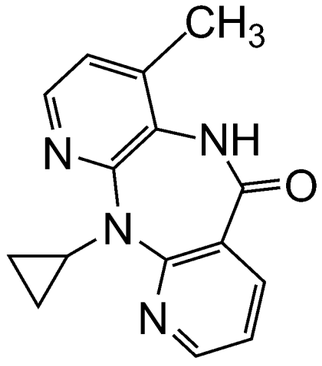

nevirapine

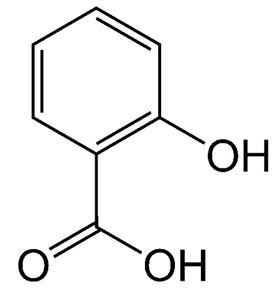

salicylic acid

Figure 1

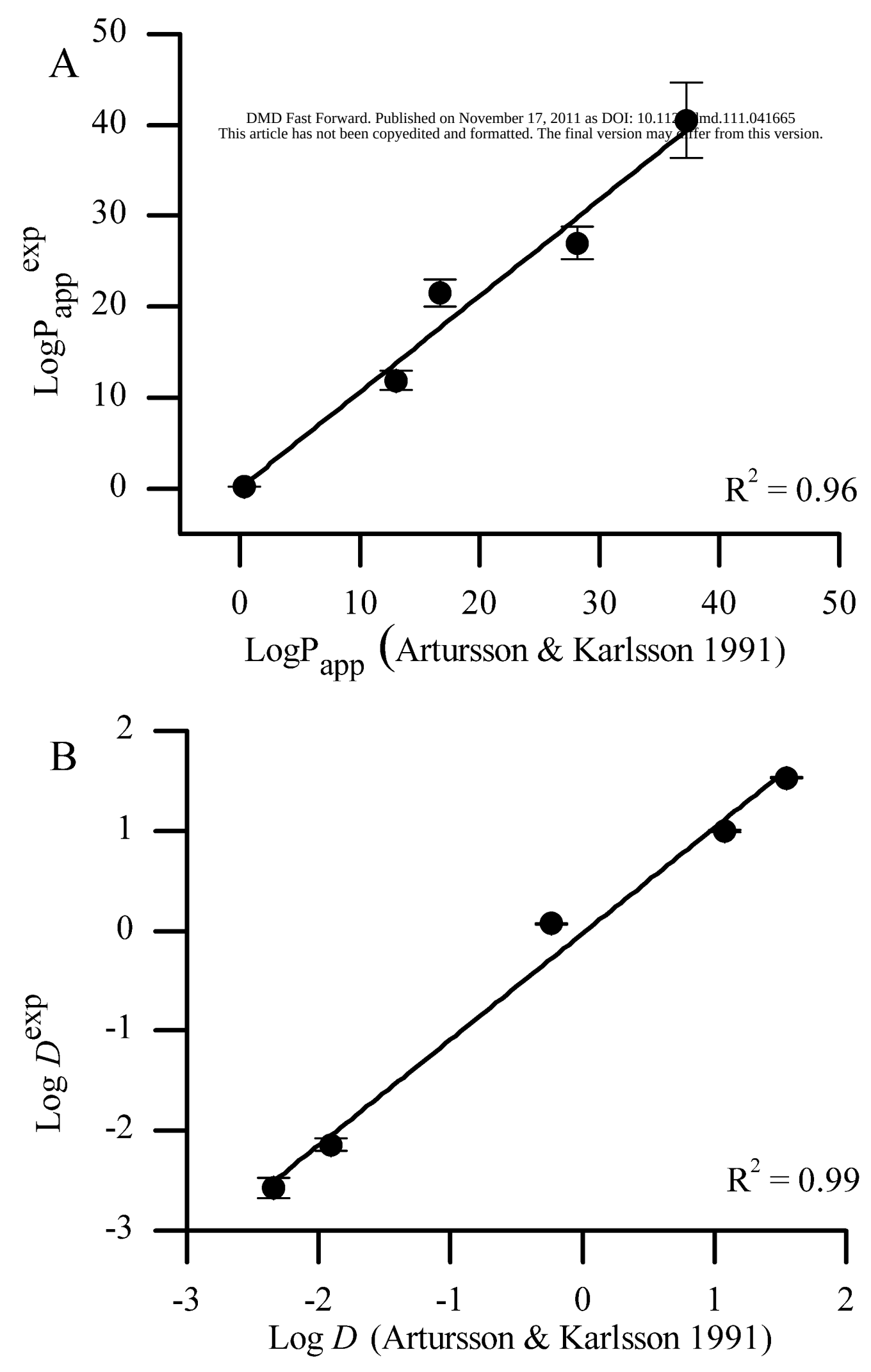

Figure 2

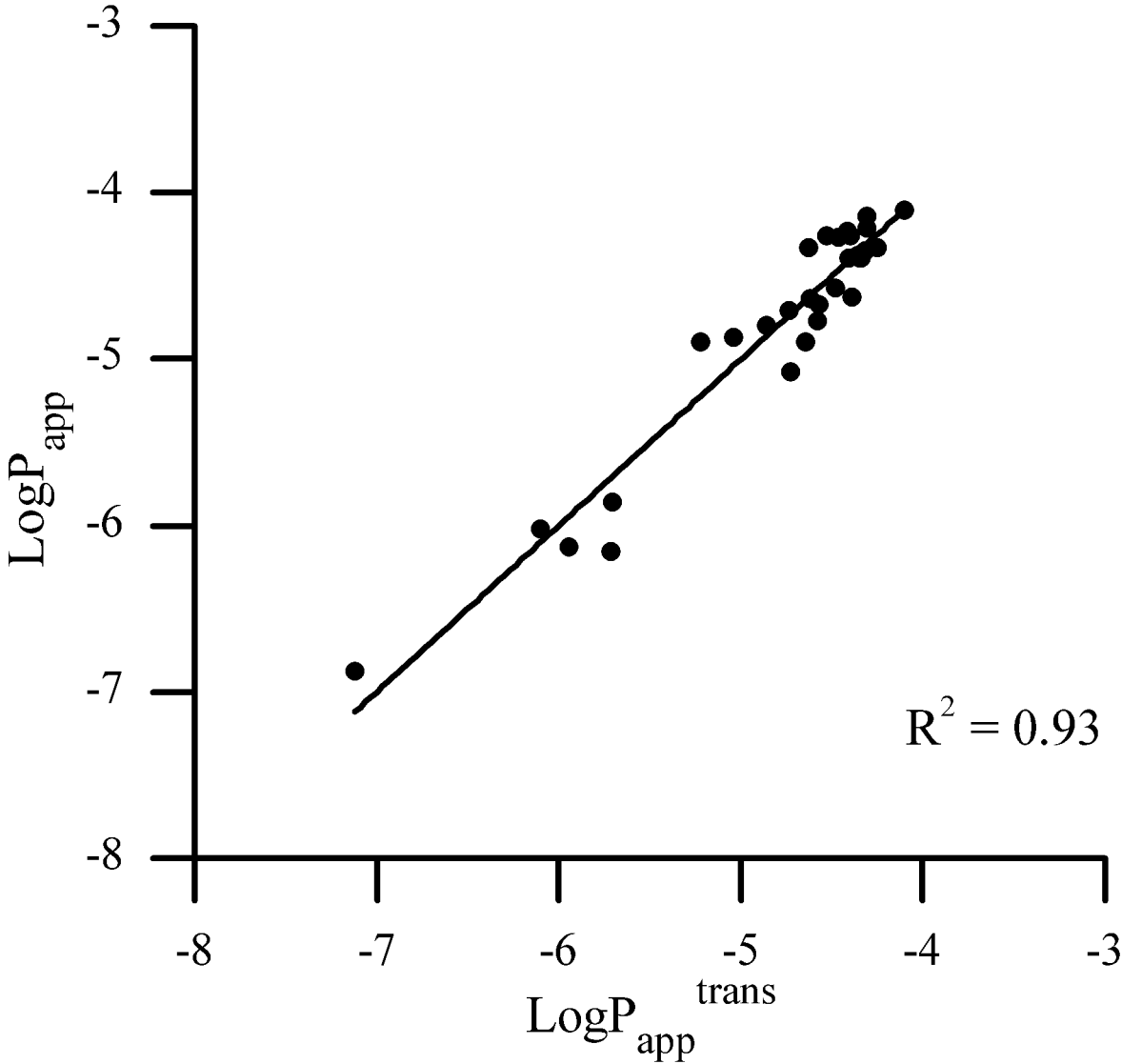

Figure 3

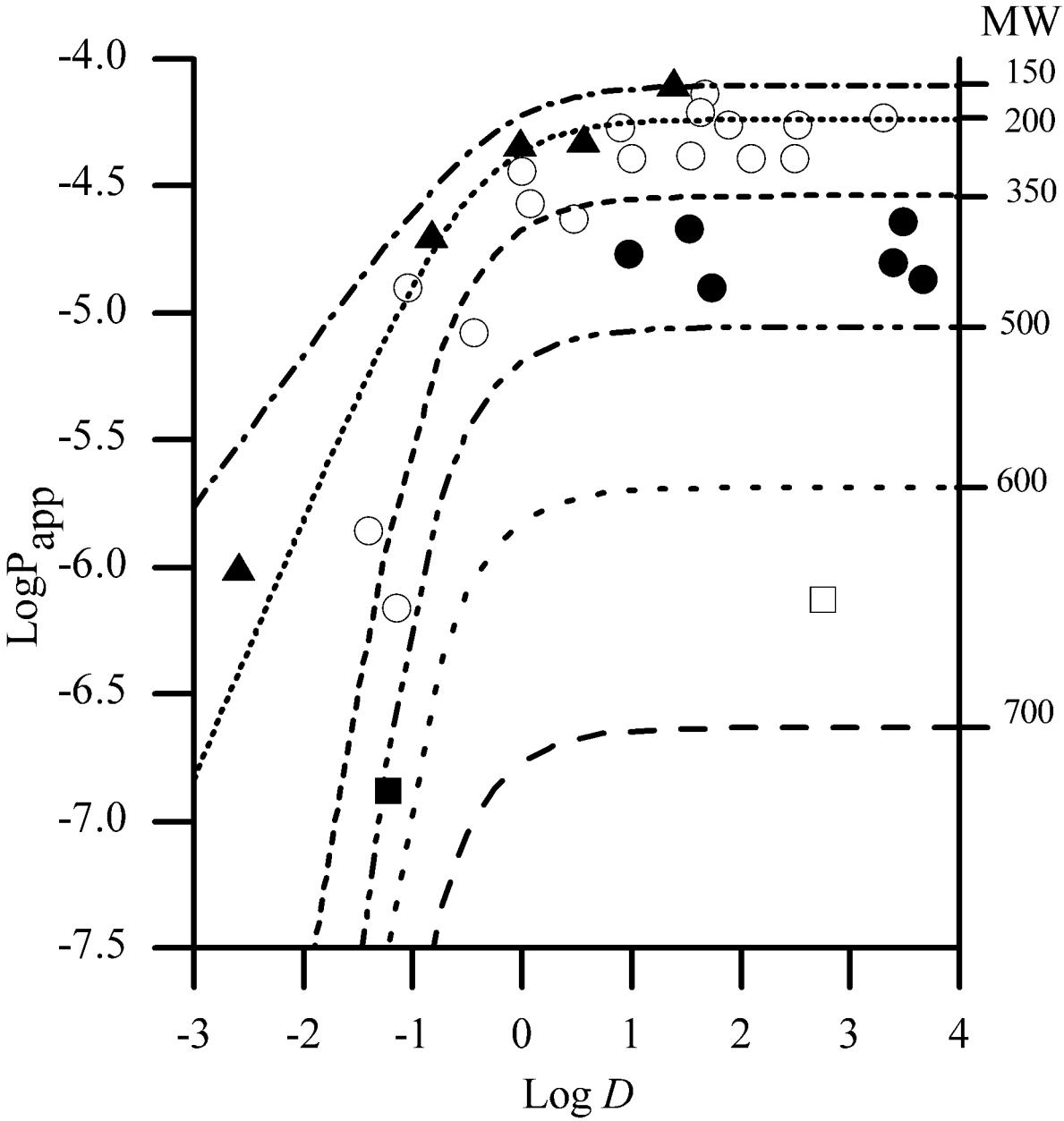
MW
150
200
350
500
600
700
-4.0
-4.5
-5.0
-5.5
-6.0
-6.5
-7.0
-7.5
LogP$_{app}$
-3
-2
-1
0
1
2
3
4
Log *D*

Figure 4

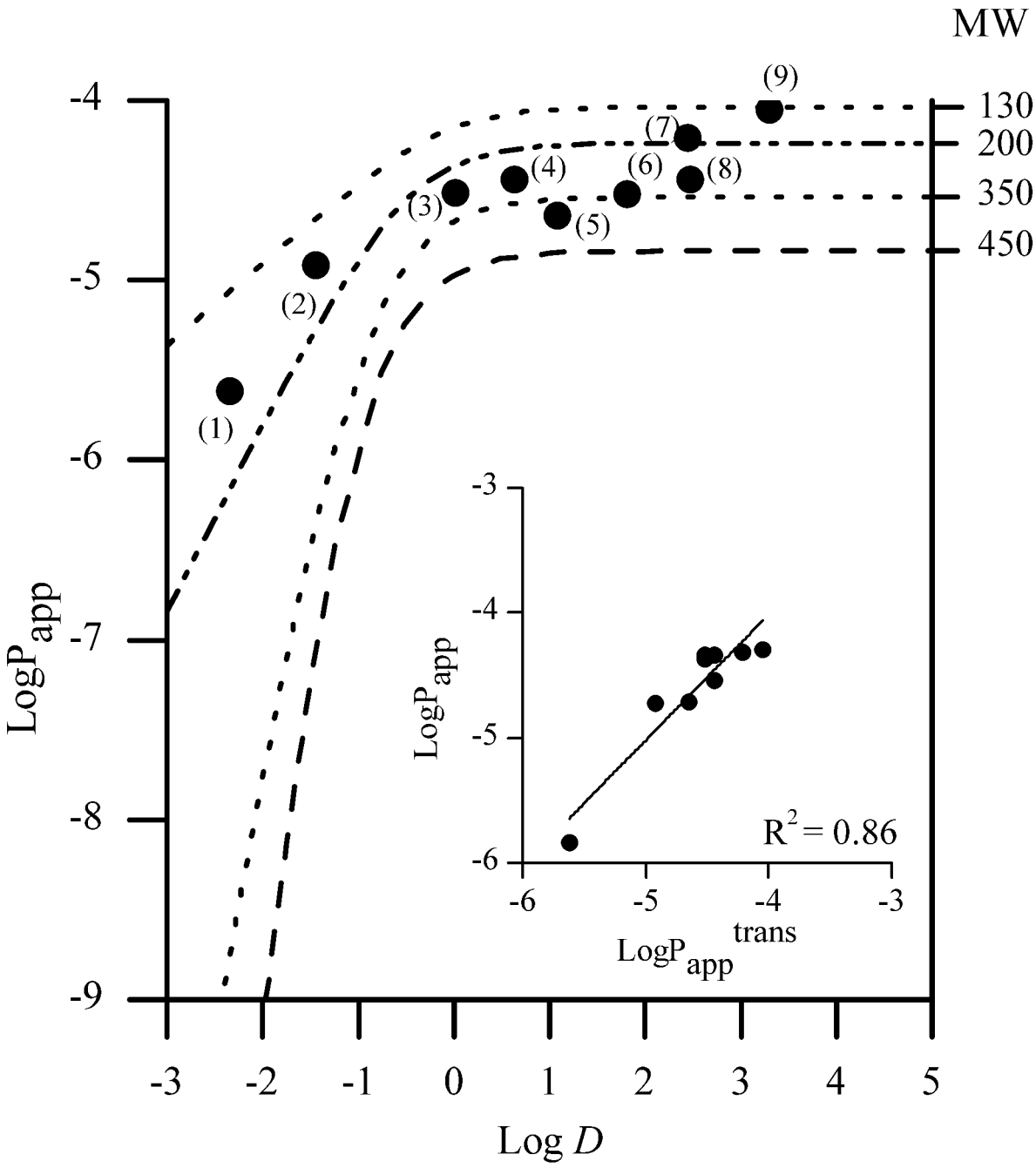
MW
130
200
350
450
(1)
(2)
(3)
(4)
(5)
(6)
(7)
(8)
(9)
-4
-5
-6
-7
-8
-9
LogP app
-3
-2
-1
0
1
2
3
4
5
Log D
-3
-4
-5
-6
LogP app
R2 = 0.86
-6
-5
-4
-3
LogP app trans

Figure 5

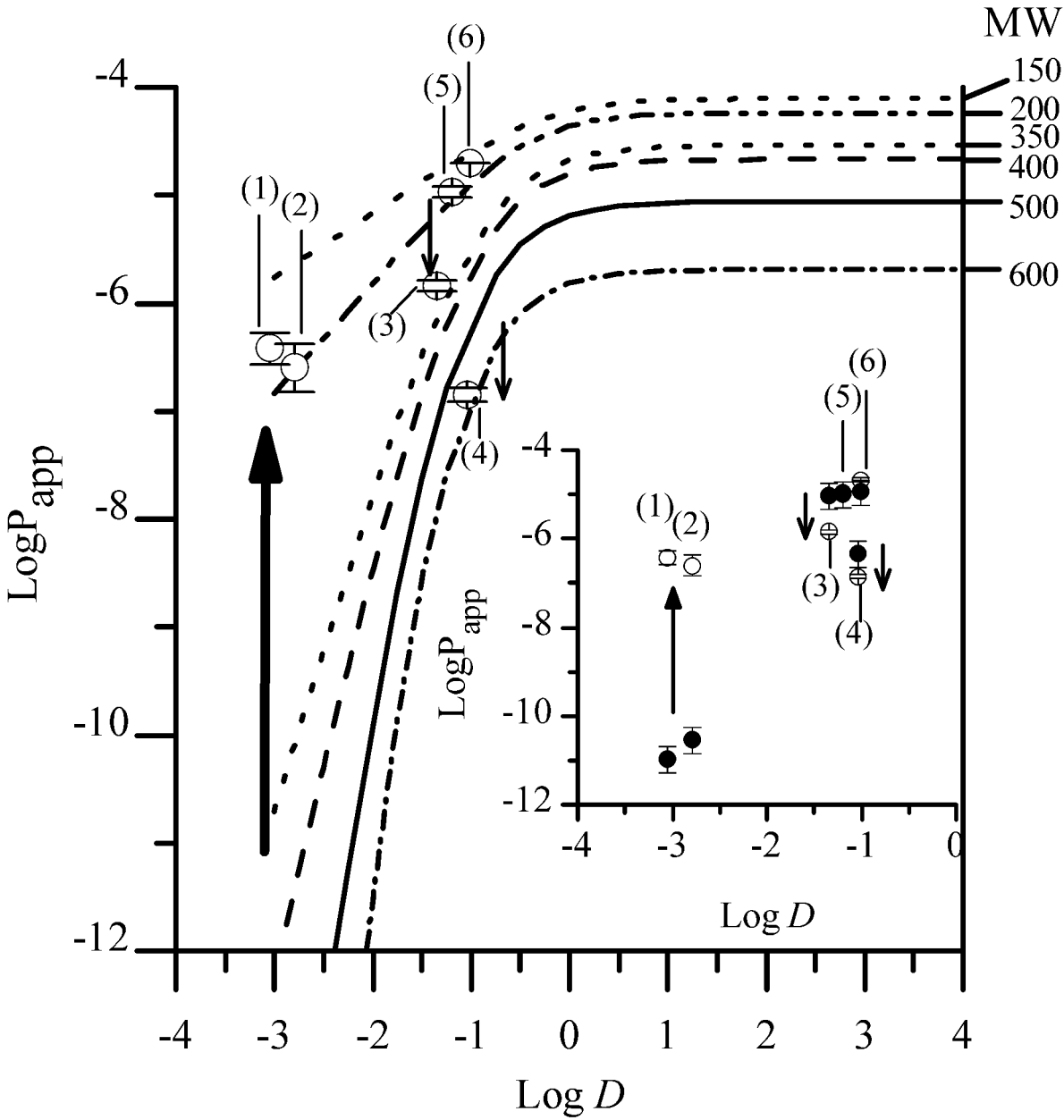
MW
150
200
350
400
500
600
(1)
(2)
(3)
(4)
(5)
(6)
LogP app
Log D
-4
-6
-8
-10
-12
-4
-3
-2
-1
0
1
2
3
4

Figure 6

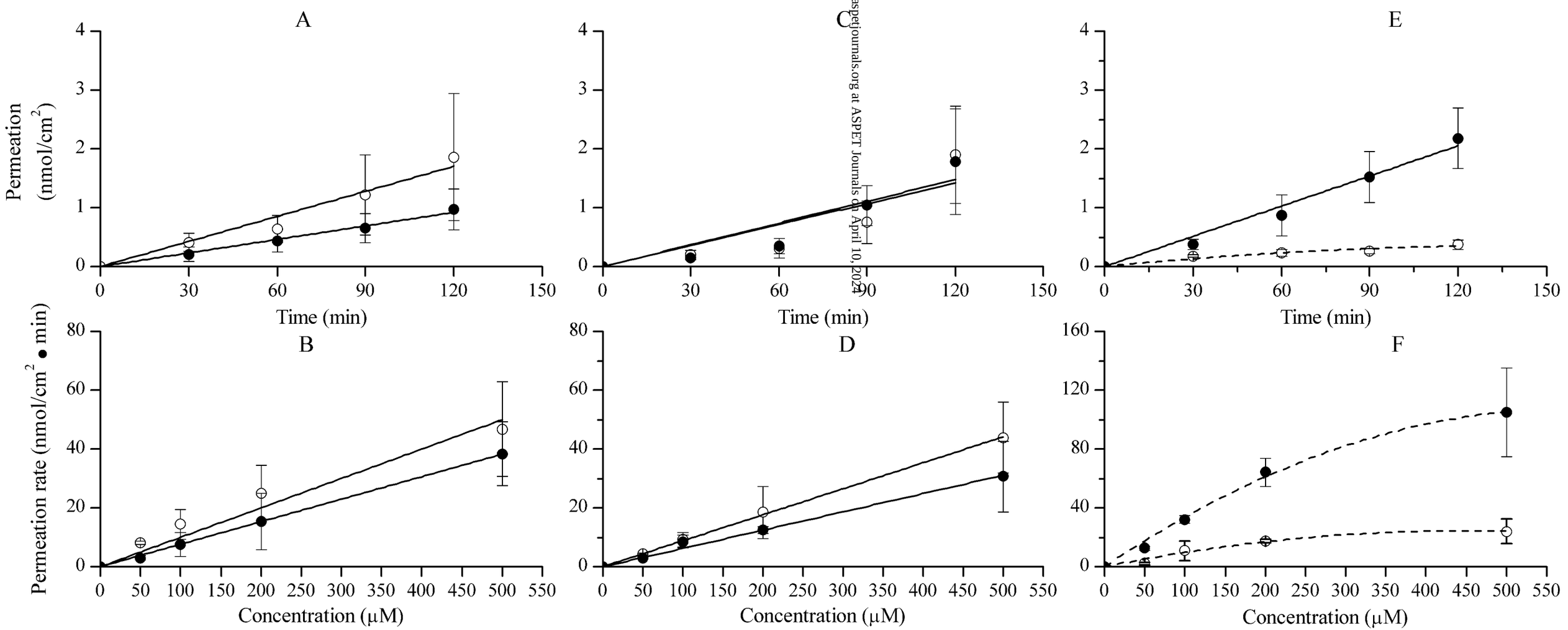

Figure 7